

Surface X-Ray Scattering during Crystal Growth: Ge on Ge(111)

E. Vlieg, A. W. Denier van der Gon, and J. F. van der Veen

*Foundation for Fundamental Research on Matter (FOM), Institute for Atomic and Molecular Physics,
Kruislaan 407, 1098 SJ Amsterdam, The Netherlands*

J. E. Macdonald

University College, Cardiff CF1 1XL, United Kingdom

C. Norris

University of Leicester, Leicester LE1 7RH, United Kingdom

(Received 26 April 1988)

The growth of Ge on Ge(111) has been monitored by *in situ* x-ray reflectivity and diffraction. For suitably chosen geometries, the scattered x-ray intensity is extremely sensitive to atomic-scale surface morphology; dramatic intensity changes occur upon deposition of a fraction of a monolayer. For substrate temperatures up to 200°C oscillations are observed in the scattered intensity, indicating growth by two-dimensional nucleation. Reflectivity curves reveal the detailed surface atomic geometry. All observations can be quantitatively understood by use of kinematical diffraction theory.

PACS numbers: 68.55.Bd, 61.10.Lx, 68.55.Jk

With the emergence of synchrotron radiation sources, x-ray diffraction has found an increasing use in the determination of surface structures.¹ This technique may also be employed to study atomic-scale surface morphology. In this Letter we report the first x-ray scattering study of the growth of a crystal by molecular-beam epitaxy. Unlike electron diffraction, for x rays multiple scattering is negligible (except very close to a bulk Bragg peak) and intensities can be computed by use of kinematical theory. This can be used to great advantage, because it allows a straightforward interpretation, not only of relative intensity changes during deposition, but also of absolute intensities needed to derive atomic positions.

The experiments were performed in the surface diffraction station of the wiggler beam line at the Synchrotron Radiation Source in Daresbury, with use of monochromatic radiation with $\lambda = 1.38 \text{ \AA}$. The setup consists of an ultrahigh-vacuum chamber coupled to a five-circle diffractometer.² The Ge(111) sample ($8 \times 8 \times 1.5 \text{ mm}^3$, $\leq 0.05^\circ$ miscut) was cleaned by repeated cycles of sputtering ($4 \times 10^{15} \text{ Ar}^+ \text{ cm}^{-2}$, 800 eV) and annealing (700°C, 15 min). After this treatment a sharp $c(2 \times 8)$ diffraction pattern is observed with the *in situ* reflection high-energy electron diffraction (RHEED) facility. A Knudsen effusion cell is used for Ge deposition with a deposition rate of $5.8 \times 10^{13} \text{ atoms cm}^{-2} \text{ min}^{-1}$ (calibrated by Rutherford backscattering).

The intensity of the specularly reflected x-ray beam was measured during Ge deposition. The angle of incidence was 6° , corresponding to destructive interference between an island on the surface and the lower-lying plane, as shown schematically in Fig. 1. In this way maximum sensitivity for islands is obtained. The data were taken for different substrate temperatures and are shown in Fig. 2. They are scaled to a starting intensity

of 100. At an angle of incidence of 6° , which is 21 times the critical angle for total reflection, the maximum reflected intensity is a factor of $\sim 10^7$ smaller than that of the incident beam.³ Typical count rates are 10 s^{-1} , with a background of 0.2 s^{-1} .

The behavior can be understood qualitatively on the basis of temperature-dependent growth modes.⁴ At room temperature (RT), the growth starts by nucleation on a flat surface. If half the surface is covered by islands, the intensity goes to zero. When deposition is continued, the intensity increases again. The period of the oscillation corresponds to the growth of one bilayer of the (111) surface ($1.4 \times 10^{15} \text{ atoms cm}^{-2}$). At a certain temperature, the diffusion length is sufficiently high for the arriving atoms to move to steps on the surface and growth proceeds by step flow. With our deposition rate this happens at 240°C and oscillations are no longer observed.

The reflected beam can be labeled as a point (hkl) in reciprocal space. We employ a hexagonal unit cell which

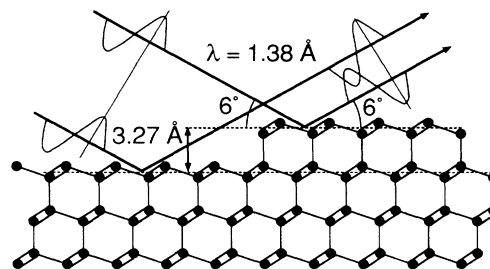


FIG. 1. Schematic showing the experimental geometry for the reflectivity measurements during Ge deposition on Ge(111). The angle of incidence is such that there is destructive interference between islands on the surface and the lower-lying plane.

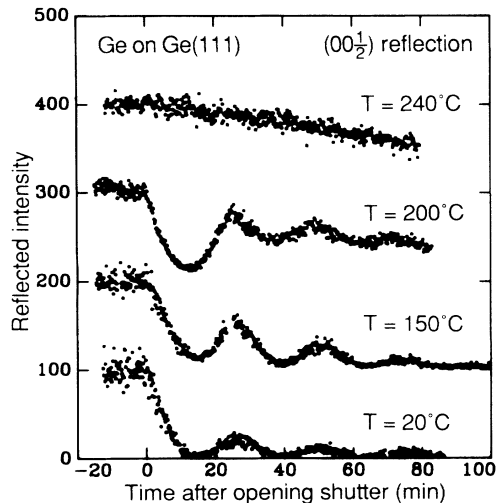


FIG. 2. The reflected signal from Ge(111) during Ge deposition. Shown are a set of curves corresponding to different substrate temperatures. The curves are normalized to a starting signal of 100 and are given vertical offsets of 100 units.

is related in reciprocal space to the conventional cubic cell by $(100)_{\text{hex}} = \frac{1}{3}(22\bar{4})_{\text{cub}}$, $(010)_{\text{hex}} = \frac{1}{3}(\bar{2}4\bar{2})_{\text{cub}}$, and $(001)_{\text{hex}} = (111)_{\text{cub}}$. Momentum transfer in the perpendicular direction is now represented by the pure index l and the specular beam at 6° angle of incidence is the $(00\frac{1}{2})$ reflection.

The in-plane crystalline quality of the deposited layers was investigated by our repeating the experiments for the $(11\frac{1}{2})$ reflection, for which there is also momentum transfer parallel to the surface. The same qualitative behavior was found: at low temperatures growth by nucleation, changing to step flow around 240°C . In Fig. 3 the result for RT growth is shown, together with data taken at an l value of 0.3. A difference with the $(00\frac{1}{2})$ data is that after opening of the shutter, there is a delay before the signal decreases. Apparently, the first arriving atoms are not located at lattice positions and only after continued deposition, a partly crystalline overlayer is formed. This is confirmed by the fact that the signal does not go to zero, again in contrast with the $(00\frac{1}{2})$ data. The delay for the $(11\frac{1}{2})$ data becomes less for increasing temperature, indicating a better crystallinity.

The results can be understood quantitatively by applying the kinematical theory of diffraction to rough surfaces. The simplest model is a one-dimensional (1D) surface with two levels for which only the contributions from the surface atoms are considered.⁵ In general, the diffracted intensity consists of two contributions: a sharp (Bragg) peak and a diffuse peak. X rays have a large penetration depth and the result for the single surface scatterer has to be multiplied by the so-called crystal truncation rod, the structure factor of which is $|F_{\text{CTR}}| = \frac{1}{2} \sin(\pi l)$.^{6,7} Ignoring constant prefactors, the

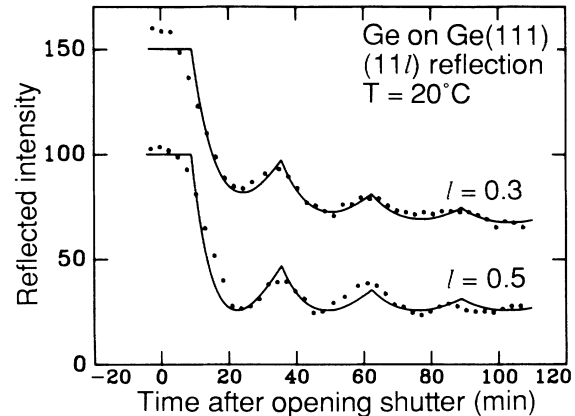


FIG. 3. The intensity of the $(11l)$ reflection during Ge deposition for two values of the perpendicular momentum transfer l . The data are normalized to a starting signal of 100, the upper data are given a vertical offset of 50 units. The solid curves are fits to the data with use of the n -level model.

result of the two-level model for x rays is

$$I_B = |F_u F_{\text{CTR}}|^2 \{1 - 2\theta(1 - \theta)[1 - \cos(2\pi l)]\} \delta(q_x), \quad (1)$$

$$I_D = |F_u F_{\text{CTR}}|^2 2\theta(1 - \theta) \times [1 - \cos(2\pi l)] [\pi L(L^{-2} + q_x^2)]^{-1}, \quad (2)$$

where F_u is the unit cell structure factor, θ is the coverage of the upper level, q_x is the momentum transfer parallel to the 1D surface, and L is the correlation length. Equations (1) and (2) have to be convoluted with the reciprocal lattice, which is equivalent to our taking, for q_x , the distance to the nearest bulk Bragg peak.

The experimental in-plane momentum transfer is two-dimensional and can be denoted by \mathbf{q}_{\parallel} . The intensity is integrated over the component of \mathbf{q}_{\parallel} which is perpendicular to the scattered beam. This effectively reduces the problem to that of a 1D surface as in Eqs. (1) and (2). The other component of \mathbf{q}_{\parallel} can then be identified with q_x . In this direction a momentum interval $\Delta q_x = 3 \times 10^{-3} \text{ \AA}^{-1}$ is accepted (for $l=0.5$), which is sufficiently large to measure I_B completely, and small enough to collect only a small part of I_D .

As a function of θ , Eq. (1) predicts, for $l=0.5$, a parabola for I_B , which is repeated after a layer is completed ($\theta=1$ corresponds to a complete bilayer). None of the measured curves shows exactly this behavior, but the first oscillation at $T=200^\circ\text{C}$ is very close to this. For $\theta=0.5$ and $l=0.5$ the Bragg intensity is zero, but the diffuse intensity has its maximum. For the RT data the intensity goes to zero, meaning that only a very small fraction of the diffuse peak is measured. Thus the correlation length and the islands on the surface are small. At higher temperatures the Ge atoms will form larger islands, corresponding to larger correlation lengths, and a larger fraction of the diffuse intensity will be collected.

The relative intensity in the first minimum of the curves for 150°C and 200°C is $\sim 15\%$. This corresponds to a correlation length of $\sim 150 \text{ \AA}$.

The two-level model does *not* explain the observed damping of the oscillations. Damping can only be explained if one takes more levels into account. Here we

will use a simple n -level model. Assume that the coverage of a certain level is a fraction f of the coverage of the previous level.⁷ If the total coverage is θ , then the coverage of level n is given by $\theta_n = \theta(1-f)^{n-1}$. We will apply this model only for RT deposition for which only the sharp Bragg peak needs to be considered. The intensity is obtained by summing over all levels:

$$I_B = |F_u F_{CTR}|^2 \left\{ [1 - \theta(1-f)]^2 + \frac{[\theta(1-f)^2]^2 + 2\theta[1 - \theta(1-f)](1-f)^2[\cos(2\pi l) - f]}{1 + f^2 - 2f \cos(2\pi l)} \right\} \delta(q_x). \quad (3)$$

The distribution over the various layers is governed by f . This distribution will be a function of the total deposition and one can take as a model $f = \theta / (\theta_{\text{half}} + \theta)$, where θ_{half} indicates the total deposition at which the surface is very rough. The lower solid curve of Fig. 3 is fitted to the data of the $(11\frac{1}{2})$ reflection for RT deposition by use of the n -level model with $\theta_{\text{half}} = 3.3$. Because of the delay in the data as discussed previously, the time origin was shifted in the fit. Also a fit for $l = 0.3$ is shown, obtained by our taking the same value for θ_{half} and only changing the l value. Thus the model gives a satisfactory description of the damping and the l dependence of the data. The deposition rate from the fits, however, is $\sim 40\%$ higher than the experimental value. This discrepancy relates to our assumption that the factor f is constant. More realistic models are currently being investigated.

The distribution of heights on the surface can be derived in more detail by the measurement of the scattered intensity along the $(00l)$ rod. The result for a freshly sputtered and annealed sample is shown by the upper points in Fig. 4. The measured intensities are multiplied by l^2 in order to account for the l dependence of the illuminated surface area and of the solid angle accepted by the detector. The solid curve through the data points in Fig. 4 is a fit with Eq. (1) with a scale factor and

keeping θ fixed at zero. Thus the sample is almost perfectly flat.

We subsequently deposited at RT Ge on the clean sample until, in the scattering geometry of Fig. 1, the first minimum in the intensity was reached (at about half a bilayer). The resulting $(00l)$ rod is shown by the lower points in Fig. 4. The dash-dotted curve is the prediction of Eq. (1) with $\theta = 0.5$ and with the same scale factor as for the annealed sample. With respect to this curve, the data are shifted to a higher l value, indicating that the effective distance of the deposited bilayer to the surface is smaller than the bulk distance. This corresponds to either a contraction of the layer spacing or to a system with both monolayer and bilayer islands. Though a contraction of the layer spacing of 5% does describe the data, it is ruled out because the same contraction should occur for the last bilayer of the clean sample, contrary to observation. The system with both monolayer and bilayer islands is modeled by assigning unequal fractional coverages θ_l and θ_h to the lower and upper half of the bilayer, respectively. We then get a three-level system: the flat bulk lattice with two layers on top. The layers are shifted with respect to each other, which can be described by the assignment of a different structure factor to each layer. The intensity is obtained by the addition of the amplitudes for the three layers and our squaring

$$I_B = |(1 - \theta_l)F_{u,\text{bulk}} + (\theta_l - \theta_h)F_{u,l} + \theta_h F_{u,h}|^2 \times |F_{CTR}|^2 \delta(q_x). \quad (4)$$

With the same scale factor as for the clean sample, the data for the deposited sample can be described by Eq. (4) with θ_l and θ_h as the fitting parameters. Note that the $(00l)$ -rod data are not sensitive to the in-plane positions of the deposited atoms. The best fit is shown in Fig. 4 by the dashed curve through the data points and is obtained for $\theta_l = 0.75$ and $\theta_h = 0.35$.⁸ Thus only half of the islands are bilayers and RT growth does not, in fact, proceed in bilayers. Clearly, the diffusivity is too small for the surface to reach its equilibrium state.

The occurrence of intensity oscillations in the specular beam during growth is well known in RHEED.^{9,10} The origin of the RHEED oscillations is still a matter of considerable debate. There is no doubt that multiple scattering is important in RHEED¹¹ and that absolute intensi-

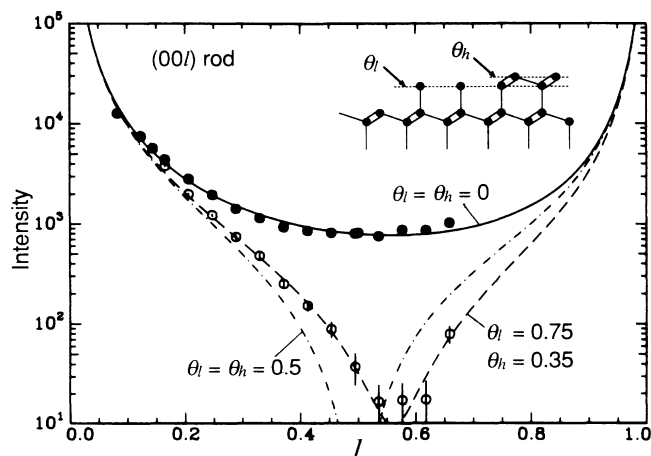


FIG. 4. The $(00l)$ rod for a freshly sputtered and annealed Ge(111) sample (filled dots), and after deposition of half a bilayer (open dots). The curves are theoretical predictions for different structure models, see text.

ties can only be derived with use of dynamical theory.¹² Therefore, one interpretation is that the oscillations are caused by multiple scattering effects from a varying step-edge density.¹³ Lent and Cohen¹⁴ assert that multiple scattering effects can be minimized by using special experimental geometries and interpret the oscillations based on diffraction from step terraces using kinematical theory.⁵

The present observation of oscillations with x rays may seem to give support to the kinematical interpretation of RHEED oscillations, but it has to be stressed that important differences occur. Aarts and Larsen⁴ studied the growth of Ge on Ge(111) using RHEED (at a much higher deposition rate). They found oscillations with monolayer period for substrate temperatures up to 180°C, changing to bilayer period up to 240°C. This is in contrast with our x-ray data, where only the bilayer period was observed. With use of an equation based on Eq. (4), it is possible to compute the intensity for pure monolayer growth on Ge(111). Even in this extreme case the kinematical theory cannot describe the monolayer amplitudes in the RHEED data.

In summary, x-ray diffraction is very sensitive to atomic-scale surface morphology, despite the large penetration depth of x rays. Provided a suitable scattering geometry is chosen, intensity changes as large as 2 orders of magnitude can be observed upon deposition of only one monolayer. Because of the applicability of kinematical theory, x-ray diffraction allows a detailed analysis of growth mode, surface morphology, and atomic geometry.

We would like to thank the Daresbury Staff, and Dr. G. Baker in particular, for their able assistance during

the measurements. Dr. P. K. Larsen is gratefully acknowledged for his advice and for providing us with the crystals. This work is part of the research program of the Stichting voor Fundamenteel Onderzoek der Materie (FOM) and is made possible by financial support from the Nederlandse Organisatie voor Wetenschappelijk Onderzoek (NWO).

¹M. Nielsen, *Z. Phys. B* **61**, 415 (1985).

²E. Vlieg, A. van't Ent, A. P. de Jongh, H. Neerings, and J. F. van der Veen, *Nucl. Instrum. Methods Phys. Res., Sect. A* **262**, 522 (1987).

³J. Als-Nielsen, *Z. Phys. B* **61**, 411 (1985).

⁴J. Aarts and P. K. Larsen, *Surf. Sci.* **188**, 391 (1987).

⁵C. S. Lent and P. I. Cohen, *Surf. Sci.* **139**, 121 (1984).

⁶S. R. Andrews and R. A. Cowley, *J. Phys. C* **18**, 6427 (1985).

⁷I. K. Robinson, *Phys. Rev. B* **33**, 3830 (1986).

⁸The (001) data are relatively insensitive to the inclusion in the model of residual adatoms from the $c(2\times 8)$ starting surface [P. M. J. Marée *et al.*, *Phys. Rev. B* **38**, 1585 (1988)].

⁹J. H. Neave, B. A. Joyce, P. J. Dobson, and N. Norton, *Appl. Phys. A* **31**, 1 (1983).

¹⁰J. M. van Hove, C. S. Lent, P. R. Pukite, and P. I. Cohen, *J. Vac. Sci. Technol. B* **1**, 741 (1983).

¹¹B. A. Joyce, P. J. Dobson, J. H. Neave, and J. Zhang, *Surf. Sci.* **174**, 1 (1986).

¹²T. Kawamura and P. A. Maksym, *Surf. Sci.* **161**, 12 (1985).

¹³P. J. Dobson, B. A. Joyce, J. H. Neave, and J. Zhang, *J. Cryst. Growth* **81**, 1 (1987).

¹⁴C. S. Lent and P. I. Cohen, *Phys. Rev. B* **33**, 8329 (1986).